



Complete assessment of whole-body n-3 and n-6 PUFA synthesis-secretion kinetics and DHA turnover in a rodent model

Adam H. Metherel,¹ R. J. Scott Lacombe, Raphaël Chouinard-Watkins, Kathryn E. Hopperton, and Richard P. Bazinet

Department of Nutritional Sciences, Faculty of Medicine, University of Toronto, Toronto, Ontario M5S 3E2, Canada

Abstract Previous assessments of the PUFA biosynthesis pathway have focused on DHA and arachidonic acid synthesis. Here, we determined whole-body synthesis-secretion kinetics for all downstream products of PUFA metabolism, including direct measurements of DHA and n-6 docosapentaenoic acid (DPAn-6, 22:5n-6) turnover, and compared n-6 and n-3 homolog kinetics. We infused labeled α -linolenic acid (ALA, 18:3n-3), linoleic acid (LNA, 18:2n-6), DHA, and DPAn-6 as $^2\text{H}_5$ -ALA, $^{13}\text{C}_{18}$ -LNA, $^{13}\text{C}_{22}$ -DHA, and $^{13}\text{C}_{22}$ -DPAn-6. Eight 11-week-old Long Evans rats fed a 10% fat diet were infused with the labeled PUFAs over 3 h, and plasma enrichment of labeled products was measured every 30 min. The DHA synthesis-secretion rate (94 ± 34 nmol/day) did not differ from other PUFA products (range, 21.8 ± 4.3 nmol/day to 408 ± 116 nmol/day). Synthesis-secretion rates of n-6 and n-3 PUFA homologs were similar, except 22:4n-6 and DPAn-6 had lower synthesis rates. However, daily turnover from newly synthesized DHA ($0.067 \pm 0.023\%$) was 56-fold to 556-fold slower than all other PUFA turnover and was 130-fold slower than that determined directly from the total plasma unesterified DHA pool. **In conclusion, n-6 and n-3 PUFA synthesis-secretion kinetics suggest that differences in turnover, not in synthesis-secretion rates, primarily determine PUFA plasma levels.**—Metherel, A. H., R. J. S. Lacombe, R. Chouinard-Watkins, K. E. Hopperton, and R. P. Bazinet. Complete assessment of whole-body n-3 and n-6 PUFA synthesis-secretion kinetics and DHA turnover in a rodent model. *J. Lipid Res.* 2018. 59: 357–367.

Supplementary key words polyunsaturated fatty acid • docosahexaenoic acid • arachidonic acid • omega-3 fatty acids • omega-6 fatty acids • fatty acid/biosynthesis • mass spectrometry

The PUFA biosynthesis pathway consists of an n-3 and n-6 arm, of which each arm is constituted by nine PUFAs that share multiple biosynthetic enzymes with other fatty acids between and within arms. To date, the majority of the literature assessing the biosynthesis pathway has focused on the synthesis of DHA from α -linolenic acid (ALA, 18:3n-3) via kinetic modeling from single doses of stable isotope tracers in humans (1–10) or kinetic modeling with stable isotope infusions in rodents (11–16). The focus on DHA synthesis from ALA is justifiable, as ALA is the largest dietary source of n-3 PUFAs (17). When ALA is considered along with DHA, the terminal n-3 PUFA in the biosynthesis pathway, they are the two most abundant n-3 PUFAs in the body. Despite this apparent need for DHA in the body, DHA synthesis rates from ALA are frequently reported to be very low in human populations (1–9, 18, 19). Furthermore, using these same conversion models, our laboratory has shown that rats yield similarly low conversion of oral doses of $^2\text{H}_5$ -ALA to plasma $^2\text{H}_5$ -DHA (11). However, we have demonstrated quantitatively that DHA synthesis-secretion rates from plasma unesterified EPA are similar to rates determined from plasma unesterified ALA (14), suggesting that when considering other precursors beyond ALA, DHA synthesis rates may be higher than previously thought.

This work was supported by Natural Sciences and Engineering Research Council of Canada Grant 482597 (R.P.B.). R.P.B. holds a Canada Research Chair in Brain Lipid Metabolism; R.J.S.L. holds an Ontario Graduate Scholarship and receives funding support through the Peterborough K. M. Hunter Charitable Foundation; R.C.W. holds a postdoctoral fellowship from the Fonds de Recherche du Québec - Santé; and K.E.H. held the Vanier Canada Graduate Scholarship. R.P.B. has received research grants from Bunge Ltd., Arctic Nutrition, the Dairy Farmers of Canada, and Nestlé Inc., as well as travel support from Mead Johnson and mass spectrometry equipment and support from Sciex. In addition, R.P.B. is on the executive committee of the International Society for the Study of Fatty Acids and Lipids and held a meeting on behalf of Fatty Acids and Cell Signaling, both of which rely on corporate sponsorship. R.P.B. has given expert testimony in relation to supplements and the brain. R.P.B. also provides complimentary fatty acid analysis for farmers, food producers, and others involved in the food industry, some of whom provide free food samples. There are no other conflicts of interest.

Manuscript received 26 October 2017 and in revised form 5 December 2017.

Published, JLR Papers in Press, December 11, 2017

DOI <https://doi.org/10.1194/jlr.M081380>

Abbreviations: ALA, α -linolenic acid; ARA, arachidonic acid; DPAn-3, n-3 docosapentaenoic acid; DPAn-6, n-6 docosapentaenoic acid; F_{PUFA} , turnover rate; GLA, γ -linolenic acid; $k_{\text{i,PUFA}}$, synthesis-secretion coefficient; LNA, linoleic acid; PFB, pentafluorobenzyl; SDA, stearidonic acid; S_{max} , maximal rate of synthesis; $t_{1/2,\text{PUFA}}$, half-life; THA, tetracosahexaenoic acid; TLE, total lipid extract; TPAn-3, n-3 tetracosapentaenoic acid; TPAn-6, n-6 tetracosapentaenoic acid; TTA, tetracosatetraenoic acid.

¹To whom correspondence should be addressed.
e-mail: adam.metherel@utoronto.ca

Although the focus has primarily been on DHA synthesis rates from ALA, many of the previously noted tracer studies have also assessed synthesis of EPA and n-3 docosapentaenoic acid (DPAn-3, 22:5n-3) from ALA, while synthesis of arachidonic acid (ARA, 20:4n-6) from linoleic acid (LNA, 18:2n-6) has also been explored (4, 5, 12, 13, 18, 19). Despite this, a more complete kinetic understanding of the synthesis and turnover of each PUFA from the essential fatty acids ALA and LNA is needed, as tissue and blood levels of these PUFAs are a balance between synthesis and turnover. For example, 24-carbon PUFAs such as tetracosahexaenoic acid (THA, 24:6n-3) and its n-6 homolog, n-6 tetracosapentaenoic acid (TPAn-6, 24:5n-6), are very rarely reported with fatty acid profiling, yet are considered to be immediate precursors to DHA and n-6 docosapentaenoic acid (DPAn-6, 22:5n-6), respectively. DHA turnover, as determined from an oral dose of ALA tracer, is higher when consuming fish (8); however, DHA turnover from an oral dose of DHA tracer following fish oil supplementation is lower (20). These conflicting findings highlight the potential limitations of measuring turnover via newly synthesized DHA from ALA. Rodent turnover of newly synthesized DHA from ALA does not change on diets ranging from 0.07% to 9.9% ALA in total fatty acids during a 3 h infusion of $^2\text{H}_5$ -ALA (13). Faster turnover of newly synthesized EPA from ALA, and not higher synthesis-secretion rates, explains the lower plasma EPA found with increased dietary LNA in rats (12). However, turnover rates determined in real-time (during 3 h infusions in rodents) from a metabolic precursor (i.e., ALA) may not truly reflect turnover, as the tracer becomes diluted and lost as it is metabolized to the various downstream products within the biosynthesis pathway. In addition, a turnover rate assessed in humans and measured in blood over hours, days, or even weeks does not take into account the contribution of adipose and tissue PUFA storage.

To address these issues, we utilize a 3 h steady-state infusion model developed by Rapoport, Igarashi, and Gao (16) and modified by our laboratory into a steady-state co-infusion model (12–14). This method minimizes the contribution of adipose and tissue storage and uptake while allowing for the determination of whole-body synthesis-secretion rates from ALA and LNA of all metabolic n-3 and n-6 PUFA products, respectively. This is the first study to utilize this protocol to measure synthesis-secretion rates and other kinetic parameters of all PUFA products following the infusion of $^2\text{H}_5$ -ALA and $^{13}\text{C}_{18}$ -LNA, and is combined with a direct real-time measure of the turnover and half-life of the terminal PUFA products, DHA and DPAn-6, following the co-infusion of $^{13}\text{C}_{22}$ -DHA and $^{13}\text{C}_{22}$ -DPAn-6. Briefly, we determined that the synthesis-secretion rate of DHA is not different from many other n-3 PUFAs, and that faster turnover is the main determinant of the low plasma abundance of fatty acids such as THA. Furthermore, a direct real-time measure of DHA turnover demonstrates that previous measures of the turnover of newly synthesized DHA were significant underestimates of direct DHA turnover.

Animals

All experimental procedures were performed in agreement with the policies set out by the Canadian Council on Animal Care and were approved by the Animal Ethics Committee at the University of Toronto. Two Long Evans dams, each with eight 18-day-old male non-littermate Long Evans pups were ordered from Charles River Laboratories (St. Constant, QC, Canada). Following arrival at the University of Toronto, the dam and pups were acclimated for 3 days and then weaned at 21 days old. The dams were placed on a DHA-free 10% fat diet with 2% ALA in total fatty acids immediately upon arriving at the University of Toronto and the pups were placed on the same diet for 8 weeks following weaning until 11 weeks of age. During this time and prior to cannulation, rats were handled frequently and housed in pairs (14).

Diets

The diet was modified from the AIN-93G custom low n-3 PUFA rodent diet (Dyets, Inc., Bethlehem, PA) (21). The diet contained 10% lipids by weight, and the fat content of the diet by weight was 32.8% safflower oil, 63.2% hydrogenated coconut oil, and 4% added fatty acid ethyl esters. The added ethyl esters were 2% oleate ethyl ester (Nu-Chek Prep, Inc., Elysian, MN) and 2% ALA ethyl ester (a gift from BASF Pharma Callanish Ltd., Isle of Lewis, UK) as the only n-3 fatty acid present in the diet. Each oil was determined to be >98% pure by GC-FID. The diet was determined previously by GC-FID to be $2.07 \pm 0.01\%$ (mean \pm SEM) by weight ALA in total fatty acids (22). Other fatty acids present included 10:0 ($4.7 \pm 0.01\%$), 12:0 ($30.8 \pm 0.2\%$), 14:0 ($12.0 \pm 0.1\%$), 16:0 ($8.5 \pm 0.02\%$), 18:0 ($8.1 \pm 0.1\%$), 18:1n-9 ($7.7 \pm 0.04\%$), and LNA ($24.7 \pm 0.1\%$).

Surgery and $^2\text{H}_5$ -ALA, $^{13}\text{C}_{22}$ -DHA, $^{13}\text{C}_{22}$ -DPAn-6, and $^{13}\text{C}_{18}$ -LNA infusion

At 8 weeks postweaning, 11-week-old rats were subjected to surgery to implant a catheter into one jugular vein and one carotid artery, as previously described in detail (12). Baseline plasma unesterified and total fatty acid concentrations were measured in plasma and drawn from the carotid artery 1 day after surgery and 2 days prior to stable isotope infusion. Modified from the method of Rapoport, Igarashi, and Gao (16), the first group of eight animals were co-infused with $0.563 \mu\text{mol}/100 \text{ g}$ body weight of $^2\text{H}_5$ -ALA (purity >95% confirmed by GC-FID and GC-MS; Cambridge Isotope Laboratories, Inc., Tewksbury, MA), $0.281 \mu\text{mol}/100 \text{ g}$ body weight of $^{13}\text{C}_{22}$ -DHA, and approximately $0.03 \mu\text{mol}/100 \text{ g}$ body weight of $^{13}\text{C}_{22}$ -DPAn-6 (Cambridge Isotope Laboratories). The second set of eight animals were infused with $2.25 \mu\text{mol}/100 \text{ g}$ body weight of $^{13}\text{C}_{18}$ -LNA (Cambridge Isotope Laboratories) only into the jugular vein for 180 min. Separate animals ($n = 8$) were used for $^{13}\text{C}_{18}$ -LNA infusion, as the $^{13}\text{C}_{22}$ -DHA also contained $^{13}\text{C}_{22}$ -DPAn-6, which could potentially have interfered with synthesis-secretion determinations from $^{13}\text{C}_{18}$ -LNA. Infusate preparation, 3 h steady-state infusions, and blood collections from the carotid artery (0, 30, 60, 90, 120, 150, and 180 min) were performed as previously described in detail (12). All blood samples were centrifuged for 15 min at 500 g (PC-100 microcentrifuge; Diamed, Mississauga, ON, Canada) and the plasma was collected and stored at -80°C .

Determination of plasma volume

Plasma volume was determined using the method of Schreihof, Hair, and Stepp (23) and modified by our laboratory (11). Briefly, a known amount of Evans Blue dye was injected into the jugular vein of a separate group of rats ($n = 3$). Fifteen minutes following injection, 1 ml of blood was drawn from the carotid

artery, twice. The plasma was collected as described above and 100 μl of plasma were diluted into 1 ml of saline. Absorbance of plasma in saline was determined at 604 nm with a Nanodrop 1000 and compared with a standard curve, and the concentration of the Evans Blue dye was determined. Concentration of the dye was then used to determine plasma volume.

Lipid extractions from baseline serum

Total lipid extracts (TLEs) for total fatty acid and for unesterified fatty acid measurements were obtained from 10 and 40 μl of serum, respectively, by a method modified from Folch, Lees, and Sloane Stanley (24). Briefly, lipids were extracted with 2:1:0.75 chloroform:methanol:0.88% potassium chloride (v:v:v) containing 1 and 4 μg of heptadecanoic acid (17:0; Nu-Chek Prep, Inc.) as internal standard for unesterified and total fatty acids, respectively. The mixtures were vortexed, centrifuged at 500 g for 10 min, and the lower chloroform lipid-containing layer was pipetted into a new test tube. TLEs for total fatty acid determinations were stored for hydrolysis as described later. TLEs for unesterified fatty acid determinations were evaporated under N_2 gas and reconstituted in 50 μl of chloroform, plated on a silica 60 G plate (Merck Millipore, Billerica, MA), and developed using TLC with 60:40:2 heptane:diethyl ether:glacial acetic acid for separation of unesterified fatty acids, as previously described (14). Unesterified fatty acids were scraped from TLC plates and extracted from the silica by the method described earlier. Isolated unesterified fatty acids were stored until derivatization to pentafluorobenzyl (PFB) esters.

Lipid extractions from stable isotope-infused plasma

TLEs were obtained from 50 μl of stable isotope-infused plasma by the Folch method, as described earlier, containing 5 μg of heptadecanoic acid (17:0; Nu-Chek Prep, Inc.) as internal standard. Four-fifths of the TLE was stored for hydrolysis and stable isotope enrichment of total fatty acids, and the remaining one-fifth of the TLE was used for isolation of isotopically labeled unesterified fatty acid by the TLC method described earlier. The isolated labeled unesterified fatty acids were stored for later derivatization to PFB esters.

Hydrolysis of total endogenous and isotopically labeled total fatty acid pools

The TLE from baseline serum and infused plasma used to determine endogenous and labeled fatty acid concentrations, respectively, was evaporated under nitrogen and the lipids were hydrolyzed in 2 ml of 10% potassium hydroxide in methanol (w:v), as previously described (10, 14, 25). Hydrolyzed fatty acids from the total lipid pool were collected and stored at -80°C for later derivatization to PFB esters.

PFB esterification

The plasma unesterified fatty acids and hydrolyzed fatty acids from total lipid pools were dried under nitrogen and derivatized to PFB esters, as previously described (10). Briefly, 100 μl of acetone:diisopropylamine:PFB bromide (1,000:10:1, v:v:v) were added and heated at 60°C for 15 min. The reagents were then evaporated under nitrogen, re-aliquoted in 40 μl of hexane, and analyzed for endogenous and labeled fatty acids by GC-MS.

Endogenous and labeled fatty acid determination by GC-MS

Fatty acid PFB esters were analyzed on an Agilent 5977A quadrupole mass spectrometer coupled to an Agilent 7890B gas chromatograph (Agilent Technologies, Mississauga, ON, Canada) in negative chemical ionization mode, as described previously (10) and recently modified by our laboratory (25). The fatty acid PFB esters were injected via an Agilent 7693 autosampler into a DB-FFAP

30 m \times 0.25 mm i.d. \times 25 μm film thickness capillary column (J&W Scientific from Agilent Technologies) interfaced directly into the ion source with helium as the carrier gas. Fatty acids were analyzed in selected ion monitoring mode using [M-H] for parent ion identification with ion dwell times of 500 μs . The [M-H] parent ions for endogenous and labeled fatty acids are presented in Table 1.

Equations

To determine the synthesis rates of n-3 PUFAs from ALA and DHA, the appearance of $^2\text{H}_5$ -PUFA and $^{13}\text{C}_{22}$ -PUFA, respectively, in the plasma-esterified pool were measured and fit to a Boltzmann sigmoidal curve ($[^2\text{H}_5/^{13}\text{C}_{22}\text{-PUFA}] \times \text{plasma volume vs. time}$) using nonlinear regression (11) (GraphPad Prism version 4.0; GraphPad Software, Inc., La Jolla, CA). In addition, the retroconversion of DHA to EPA, as measured by the appearance of $^{13}\text{C}_{20}$ -EPA, was included in our calculations. At any point on the curves, the slope (S) is determined by the ability of the body to synthesize $^2\text{H}_5$ -PUFA from $^2\text{H}_5$ -ALA or $^{13}\text{C}_{22}$ -PUFA from $^{13}\text{C}_{22}$ -DHA and the ability of the periphery to uptake $^2\text{H}_5$ -PUFA (equation 1) or $^{13}\text{C}_{22}$ -PUFA (equation 2), respectively. Identical calculations to determine synthesis rates of n-6 PUFAs from LNA and DPAn-6 were also implemented (equations 3 and 4).

$$S = k_{1,\text{PUFA}} \left[^2\text{H}_5\text{-ALA} \right]_{\text{unesterified}} - k_{1,\text{PUFA}} \left[^2\text{H}_5\text{-PUFA} \right]_{\text{esterified}} \quad (\text{Eq. 1})$$

$$S = k_{1,\text{PUFA}} \left[^{13}\text{C}_{22}\text{-DHA} \right]_{\text{unesterified}} - k_{1,\text{PUFA}} \left[^{13}\text{C}_{22}\text{-PUFA} \right]_{\text{esterified}} \quad (\text{Eq. 2})$$

$$S = k_{1,\text{PUFA}} \left[^{13}\text{C}_{18}\text{-LNA} \right]_{\text{unesterified}} - k_{1,\text{PUFA}} \left[^{13}\text{C}_{18}\text{-PUFA} \right]_{\text{esterified}} \quad (\text{Eq. 3})$$

$$S = k_{1,\text{PUFA}} \left[^{13}\text{C}_{22}\text{-DPAn-6} \right]_{\text{unesterified}} - k_{1,\text{PUFA}} \left[^{13}\text{C}_{22}\text{-PUFA} \right]_{\text{esterified}} \quad (\text{Eq. 4})$$

where $k_{1,\text{PUFA}}$ is the steady-state synthesis-secretion coefficient for any PUFA, representing a measure for the amount of infused label that is converted to downstream products, $[^2\text{H}_5\text{-ALA}]_{\text{unesterified}}$, $[^{13}\text{C}_{22}\text{-DHA}]_{\text{unesterified}}$, $[^{13}\text{C}_{18}\text{-LNA}]_{\text{unesterified}}$, and $[^{13}\text{C}_{22}\text{-DPAn-6}]_{\text{unesterified}}$ are the plasma concentrations of the infusate, $k_{1,\text{PUFA}}$ is the disappearance coefficient for any individual PUFA, and $[^2\text{H}_5/^{13}\text{C}_{22}/^{13}\text{C}_{18}\text{-PUFA}]_{\text{esterified}}$ is the concentration of an individual PUFA in the plasma that has been synthesized from the respective infusate, packaged into lipoprotein, and secreted into the plasma.

The maximum first derivative or maximal rate of synthesis (S_{max}) of the curves is assumed to be the time point when the uptake of esterified labeled PUFAs from the periphery is negligible, i.e., zero (equations 5–8).

$$S_{\text{max}} = k_{1,\text{PUFA}} \left[^2\text{H}_5\text{-ALA} \right]_{\text{unesterified}} - 0 \quad (\text{Eq. 5})$$

$$S_{\text{max}} = k_{1,\text{PUFA}} \left[^{13}\text{C}_{22}\text{-DHA} \right]_{\text{unesterified}} - 0 \quad (\text{Eq. 6})$$

$$S_{\text{max}} = k_{1,\text{PUFA}} \left[^{13}\text{C}_{18}\text{-LNA} \right]_{\text{unesterified}} - 0 \quad (\text{Eq. 7})$$

$$S_{\text{max}} = k_{1,\text{PUFA}} \left[^{13}\text{C}_{22}\text{-DPAn-6} \right]_{\text{unesterified}} - 0 \quad (\text{Eq. 8})$$

Therefore, the derivative at this point is equal to the rate of $^2\text{H}_5$ -PUFA, $^{13}\text{C}_{18}$ -PUFA, or $^{13}\text{C}_{22}$ -PUFA synthesis-secretion. By correcting the S_{max} by the substrate tracer:tracer ratio, the rates of actual PUFA synthesis are determined, $J_{\text{syn,PUFA}}$ (nanomoles per minute) (11).

$$J_{\text{syn,PUFA}} = S_{\text{max}} \left(\left[\text{ALA} \right]_{\text{unesterified}} / \left[^2\text{H}_5\text{-ALA} \right]_{\text{unesterified}} \right) \\ = k_{1,\text{PUFA}} \left[\text{ALA} \right]_{\text{unesterified}} \quad (\text{Eq. 9})$$

TABLE 1. Detected masses of PUFA-PFB esters by negative chemical ionization

Fatty Acid	PUFA	² H ₅ PUFA	¹³ C ₂₀₋₂₂ PUFA	¹³ C ₁₈ PUFA
ALA	277.4	282.4	—	—
SDA	275.4	280.4	—	—
20:3n-3	305.4	310.4	—	—
20:4n-3	303.4	308.4	—	—
EPA	301.4	306.4	321.4	—
DPAAn-3	329.4	334.4	—	—
DHA	327.4	332.4	349.4	—
TPAn-3	357.4	362.4	—	—
THA	355.4	360.4	—	—
LNA	279.4	—	—	297.4
GLA	277.4	—	—	295.4
20:2n-6	307.4	—	—	325.4
DGLA	305.4	—	—	323.4
ARA	303.4	—	323.4	321.4
22:4n-6	331.4	—	—	349.4
DPAAn-6	329.4	—	351.4	347.4
TTA	359.4	—	—	377.4
TPAn-6	357.4	—	—	375.4

Detected masses represent parent ion with a negative charge (M-1). DGLA, dihomo- γ -linolenic acid;

$$J_{syn,PUFA} = S_{max} \left(\frac{[DHA]_{unesterified}}{[^{13}C_{22}\text{-DHA}]_{unesterified}} \right) \quad (Eq. 10)$$

$$= k_{1,PUFA} [DHA]_{unesterified}$$

$$J_{syn,PUFA} = S_{max} \left(\frac{[LNA]_{unesterified}}{[^{13}C_{18}\text{-LNA}]_{unesterified}} \right) \quad (Eq. 11)$$

$$= k_{1,PUFA} [LNA]_{unesterified}$$

$$J_{syn,PUFA} = S_{max} \left(\frac{[DPAAn-6]_{unesterified}}{[^{13}C_{22}\text{-DPAAn-6}]_{unesterified}} \right) \quad (Eq. 12)$$

$$= k_{1,PUFA} [DPAAn-6]_{unesterified}$$

The diet consumed for this study contained no PUFAs other than ALA and LNA, therefore it can be assumed that the plasma total PUFAs were constant during the infusion period. Therefore, the turnover rate (F_{PUFA}) and half-life ($t_{1/2,PUFA}$) of total PUFAs in the plasma can be determined by equations 13 and 14, respectively.

$$F_{PUFA} = J_{syn,PUFA} / (V_{plasma} \times [PUFA]_{esterified}) \quad (Eq. 13)$$

$$t_{1/2,PUFA} = 0.693 / F_{PUFA} \quad (Eq. 14)$$

Statistics

Differences in n-3 PUFA synthesis rates from ALA and n-6 PUFA synthesis rates from LNA were assessed by one-way ANOVA followed by Tukey's HSD post hoc test. Student's *t*-test was used to compare kinetic parameters located at the same enzymatic step between n-3 and n-6 PUFA pathways determined from ALA and LNA precursors, respectively, as well as kinetic parameters of DPAAn-6 synthesis-secretion from LNA versus DPAAn-6. Paired *t*-test was used to compare kinetic parameters of DHA and EPA synthesis-secretion parameters from ALA versus DHA. Normality was assessed by the Shapiro-Wilk test for normality and, in the case of nonnormally distributed groups, the data were log transformed prior to statistical analysis. All data are presented as mean \pm SEM.

RESULTS

Plasma PUFA concentrations

Plasma total fatty acid concentrations were determined for all n-3 and n-6 PUFAs in the biosynthesis pathways (Fig. 1). Plasma total n-3 PUFAs ranged from as low as 0.22 ± 0.02

nmol/ml of n-3 tetracosapentaenoic acid (TPAn-3, 24:5n-3) and 0.44 ± 0.07 nmol/ml of stearidonic acid (SDA, 18:4n-3) to 181 ± 26 nmol/ml of DHA. A similar, but larger, range in total plasma n-6 PUFAs was shown from 0.67 ± 0.03 nmol/ml of tetracosatetraenoic acid (TTA, 24:4n-6) and 1.7 ± 0.2 nmol/ml of TPAn-6 to $1,498 \pm 88$ nmol/ml and $1,473 \pm 112$ nmol/ml of LNA and ARA, respectively. Plasma unesterified fatty acid concentrations were determined to be 144 ± 14 nmol/ml for LNA, 3.6 ± 0.4 nmol/ml for ALA, 0.8 ± 0.1 nmol/ml for DPAAn-6, and 1.9 ± 0.2 nmol/ml for DHA (Fig. 2A).

Blood samples collected throughout the stable isotope infusion from 30, 60, 90, 120, 150, and 180 min were used to determine the average exposure levels and these values were subsequently used in equations 1–12. The average plasma unesterified concentrations of the infused isotopes were 3.3 ± 0.3 nmol/ml for ¹³C₁₈-LNA, 0.67 ± 0.09 nmol/ml for ²H₅-ALA, 0.008 ± 0.001 nmol/ml for ¹³C₂₂-DPAAn-6, and 0.05 ± 0.01 nmol/ml for ¹³C₂₂-DHA (Fig. 2B). Specific activities (Fig. 2C) determined as the ratio of the labeled infusate to the endogenous unesterified fatty acid pool were then determined to be 0.025 ± 0.003 , 0.23 ± 0.06 , 0.012 ± 0.003 , and 0.033 ± 0.008 for LNA, ALA, DPAAn-6, and DHA, respectively.

The n-3 PUFA synthesis-secretion coefficients, rates, turnover rates, and half-life

Synthesis-secretion parameters were determined for maximal rate of synthesis (S_{max} , nanomoles per minute), synthesis-secretion coefficient ($k_{1,PUFA}$, nanomoles per minute), daily synthesis-secretion rates (nanomoles per day), turnover (percent per day), and half-life (days) for all n-3 and n-6 PUFAs in the biosynthesis pathways (Table 2). Representative GC-MS chromatograms are presented for ²H₅-TPAn-3 and ²H₅-THA (Fig. 3A) and for ²H₅-DHA (Fig. 3C) and ¹³C₂₂-DHA (Fig. 3B). Representative infusion curves and maximum first derivatives (S_{max}) are also presented for the synthesis-secretion of minor (Fig. 4A) and major (Fig. 4B) n-3 PUFA products and for the infused labeled fatty acid (Fig. 4C).

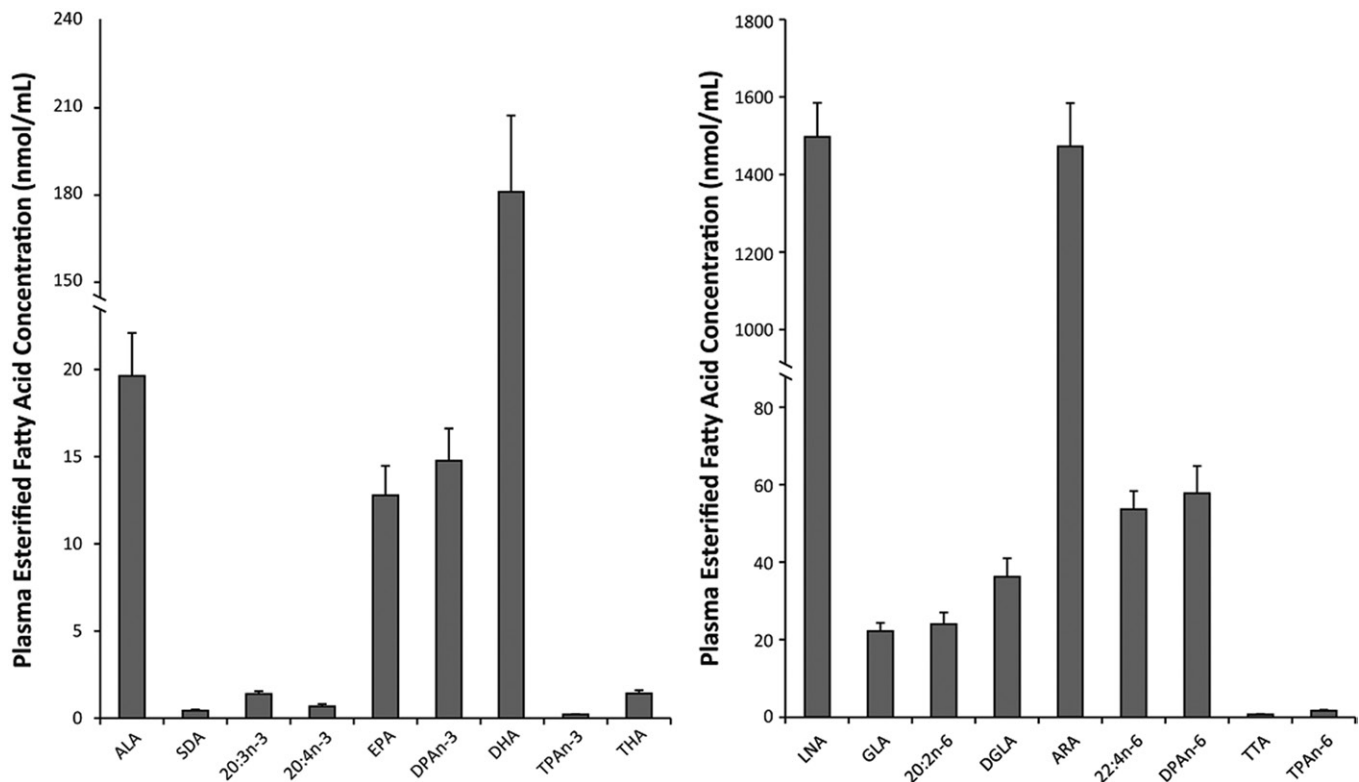


Fig. 1. Baseline esterified fatty acid concentrations for all n-3 and n-6 PUFAs in male Long Evans rats following an 8 week 2% ALA diet. Values are expressed as mean \pm SEM, $n = 8$. DGLA, dihomog- γ -linolenic acid;

In the n-3 PUFA pathway, SDA, TPAAn-3, and THA represent the lowest synthesis-secretion coefficients and daily synthesis-secretion rates from ALA. These synthesis-secretion coefficients were between 8- and 72-fold lower than those determined for 20:4n-3, EPA, and DPAn-3, although SDA and THA were not different than DHA. Similarly, synthesis-secretion rates from ALA for SDA, TPAAn-3, and THA were all lower ($P < 0.05$) than EPA and DPAn-3 by between 4- and 53-fold. Interestingly, daily synthesis-secretion rates were not different between DHA, THA, and SDA. The turnover of DHA from ALA was slower ($P < 0.05$) compared with all other n-3 PUFAs in the pathway, and conversely, the half-life was longest for DHA from ALA. However, when determining turnover and half-life of DHA more directly from $^{13}\text{C}_{22}$ -DHA infusate, turnover was more than 130-fold faster ($P < 0.05$) and the half-life more than 200-fold shorter than when determined from $^2\text{H}_5$ -ALA.

The n-6 PUFA synthesis-secretion coefficients, rates, turnover rates, and half-life

Synthesis-secretion parameters were determined for maximal rate of synthesis, synthesis-secretion coefficient, daily synthesis-secretion rate, turnover, and half-life for all n-6 PUFAs in the biosynthesis pathways (Table 2). In the n-6 pathway, maximal rate of synthesis, synthesis-secretion coefficient, and the daily synthesis-secretion rate for DPAn-6 from LNA were lower ($P < 0.05$) compared with all other downstream n-6 PUFA products of LNA, except when compared with 20:2n-6. Furthermore, 20:2n-6 demonstrates lower ($P < 0.05$) values for the aforementioned

kinetic parameters when compared with ARA and 22:4n-6. Turnover from LNA was slower and the half-life longer ($P < 0.05$) for ARA and DPAn-6 compared with all other n-6 PUFAs. However, similar to the n-3 PUFA pathway, when determining turnover and half-life of DPAn-6 more directly from $^{13}\text{C}_{22}$ -DPAn-6 infusate, turnover was more than 90-fold faster ($P < 0.05$) and the half-life 45-fold shorter than when determined from $^{13}\text{H}_{18}$ -LNA, again demonstrating how previous turnover and half-life values by this model have been under- and overestimated, respectively. Kinetic parameters for retroconversion of DPAn-6 to ARA and synthesis-secretion of TTA and TPAAn-6 from LNA were not detectable.

A comparison of kinetic parameters between n-3 and n-6 PUFA pathways

The synthesis-secretion coefficient for all n-3 PUFAs in the biosynthesis pathway were higher ($P < 0.05$) compared with all n-6 PUFA homologs. For example, EPA and ARA, which are located in the same position of the n-3 and n-6 PUFA pathway, respectively, yielded synthesis-secretion coefficient values of 0.068 ± 0.013 ml/min (mean \pm SEM) for EPA from ALA that were higher ($P < 0.05$) than the 0.003 ± 0.001 ml/min for ARA from LNA. Interestingly, the daily synthesis-secretion rates were 14- and 15-fold higher for LNA and γ -linolenic acid (GLA, 18:3n-6) compared with ALA and SDA, respectively, and the DPAn-6 rate was lower than DHA with no other differences between the two pathways. For all n-3 PUFAs from ALA to EPA in the pathway, turnover was

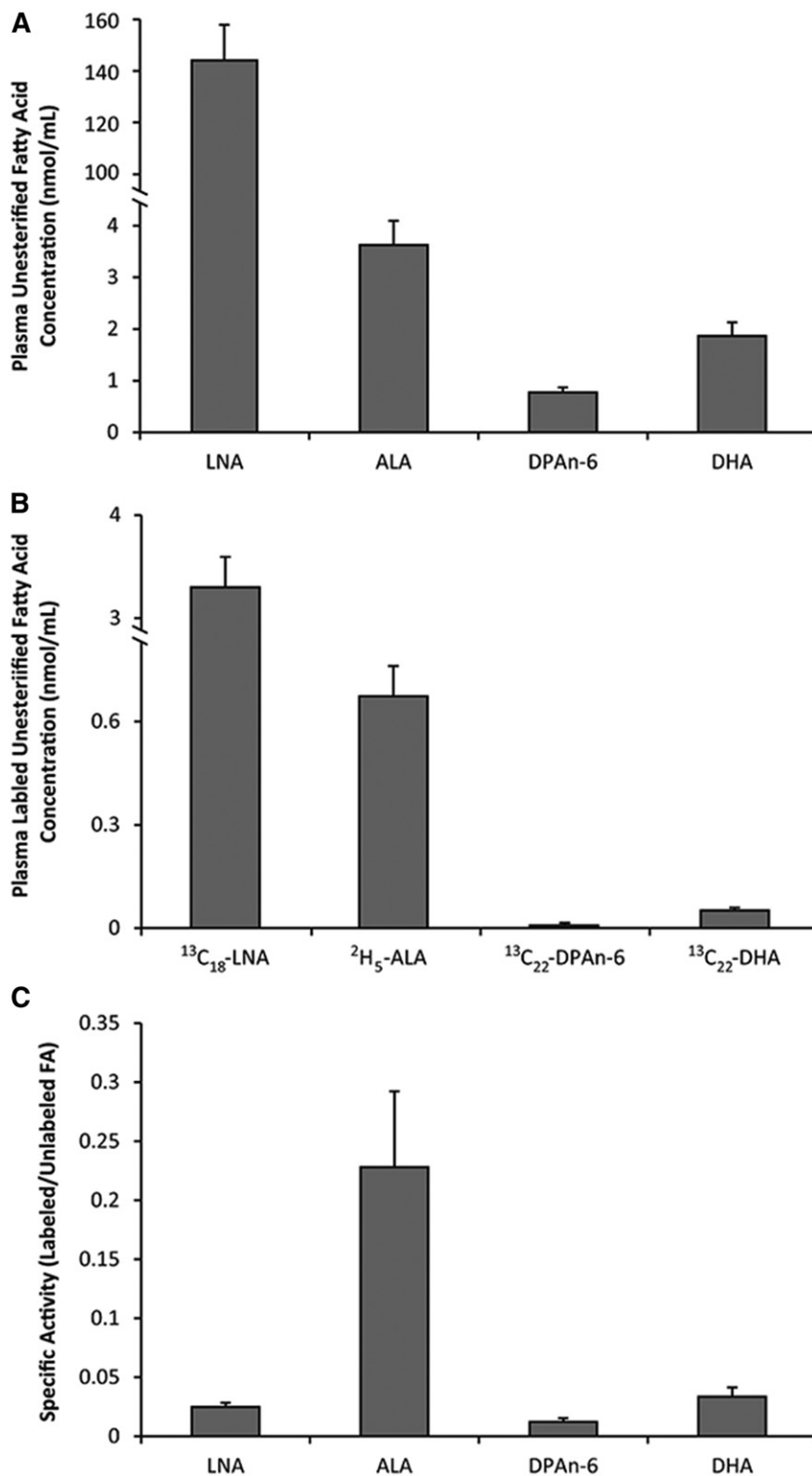


Fig. 2. Baseline plasma unesterified fatty acid concentrations (A), unesterified labeled fatty acid infusate concentrations (B), and specific activities for infused PUFAs in male Long Evans rats following an 8 week 2% ALA diet (C). Values are expressed as mean \pm SEM, n = 8.

faster and half-life was shorter compared with the respective n-6 PUFA homologs, after which DPAn-3 and DHA turnover and half-life were not different ($P > 0.05$) compared with 22:4n-6 and DPAn-6, respectively. The maximal rate of synthesis, synthesis-secretion coefficient, and daily

synthesis-secretion rate of unesterified DHA into total DHA were 13-, 1.6-, and 6-fold higher ($P < 0.05$) than unesterified DPAn-6 into total DPAn-6; however, no differences ($P > 0.05$) in turnover or half-life were determined between DHA and DPAn-6.

TABLE 2. Kinetic parameters for all n-3 and n-6 PUFA whole-body synthesis-secretion following infusion of $^3\text{H}_5\text{-ALA}$, $^{13}\text{C}_{22}\text{-DHA}$, $^{13}\text{C}_{18}\text{-LNA}$, and $^{13}\text{C}_{22}\text{-DPAn-6}$ over 3 h

Tracer Source	Fatty Acid	Maximal Rate of Synthesis (S_{max} , nmol/min)	Synthesis-Secretion Coefficient ($k_{1,\text{PUFA}}$, ml/min)	Daily Synthesis-Secretion Rate (nmol/day)	Turnover (F_{PUFA} , %/day)	Half-Life ($t_{1/2,\text{PUFA}}$, days)
n-3 PUFA pathway						
ALA	ALA	$0.24 \pm 0.04^{\text{a}}$	$0.37 \pm 0.05^{\text{a}}$	$1971 \pm 393^{\text{a}}$	$12.8 \pm 2.1^{\text{ab}}$	$0.068 \pm 0.013^{\text{ab}}$
	SDA	$0.003 \pm 0.001^{\text{de}}$	$0.004 \pm 0.001^{\text{de}}$	$21.8 \pm 4.3^{\text{de}}$	$8.4 \pm 2.5^{\text{ab}}$	$0.16 \pm 0.05^{\text{ab}}$
	20:3n-3	$0.012 \pm 0.004^{\text{cd}}$	$0.019 \pm 0.007^{\text{cd}}$	$92.8 \pm 24.3^{\text{bcd}}$	$8.7 \pm 2.8^{\text{ab}}$	$0.19 \pm 0.07^{\text{ab}}$
	20:4n-3	$0.021 \pm 0.007^{\text{bc}}$	$0.035 \pm 0.012^{\text{bc}}$	$203 \pm 75^{\text{bc}}$	$37.3 \pm 12.8^{\text{a}}$	$0.035 \pm 0.009^{\text{a}}$
	EPA	$0.040 \pm 0.007^{\text{b}}$	$0.068 \pm 0.013^{\text{b}}$	$369 \pm 86^{\text{b}}$	$3.9 \pm 0.9^{\text{b}}$	$0.38 \pm 0.15^{\text{b}}$
	DPAn-3	$0.043 \pm 0.009^{\text{b}}$	$0.072 \pm 0.017^{\text{b}}$	$408 \pm 116^{\text{b}}$	$4.0 \pm 1.1^{\text{b}}$	$0.89 \pm 0.67^{\text{b}}$
	TPAn-3	$0.001 \pm 0.0001^{\text{e}}$	$0.001 \pm 0.0001^{\text{e}}$	$7.6 \pm 1.4^{\text{e}}$	$5.1 \pm 1.1^{\text{b}}$	$0.34 \pm 0.20^{\text{b}}$
	THA	$0.004 \pm 0.001^{\text{d}}$	$0.007 \pm 0.002^{\text{de}}$	$42.1 \pm 12.9^{\text{de}}$	$3.8 \pm 1.0^{\text{b}}$	$0.78 \pm 0.50^{\text{b}}$
	DHA	$0.011 \pm 0.003^{\text{cd}}$	$0.017 \pm 0.005^{\text{cd}}$	$94 \pm 31.4^{\text{bcd}}$	$0.067 \pm 0.023^{\text{c}}$	$30.4 \pm 11.6^{\text{c}}$
DHA	EPA	$0.006 \pm 0.001^{\text{f}}$	$0.13 \pm 0.03^{\text{f}}$	373 ± 121	4.3 ± 1.6	0.31 ± 0.07
	DHA	$0.18 \pm 0.03^{\text{f}}$	$4.2 \pm 0.9^{\text{f}}$	$11780 \pm 3147^{\text{f}}$	$8.9 \pm 2.4^{\text{f}}$	$0.14 \pm 0.04^{\text{f}}$
n-6 PUFA pathway						
LNA	LNA	$0.427 \pm 0.044^{\text{a,*}}$	$0.137 \pm 0.018^{\text{a,*}}$	$28695 \pm 4715^{\text{a,*}}$	$2.6 \pm 0.4^{\text{a,*}}$	$0.31 \pm 0.04^{\text{a,*}}$
	GLA	$0.005 \pm 0.001^{\text{bc,*}}$	$0.002 \pm 0.0003^{\text{bc,*}}$	$343 \pm 72^{\text{bc,*}}$	$2.7 \pm 1.0^{\text{ab,*}}$	$0.92 \pm 0.59^{\text{ab,*}}$
	20:2n-6	$0.0014 \pm 0.0003^{\text{cd,*}}$	$0.0005 \pm 0.0001^{\text{cd,*}}$	$98 \pm 25^{\text{cd}}$	$0.67 \pm 0.22^{\text{b,*}}$	$2.8 \pm 1.1^{\text{b,*}}$
	DGLA	$0.009 \pm 0.003^{\text{bc,*}}$	$0.003 \pm 0.001^{\text{bc,*}}$	$446 \pm 130^{\text{bc}}$	$1.7 \pm 0.4^{\text{ab,*}}$	$0.73 \pm 0.23^{\text{ab,*}}$
	ARA	$0.011 \pm 0.005^{\text{b,*}}$	$0.003 \pm 0.001^{\text{b,*}}$	$610 \pm 205^{\text{b}}$	$0.056 \pm 0.018^{\text{c,*}}$	$23 \pm 7^{\text{c,*}}$
	22:4n-6	$0.017 \pm 0.01^{\text{b,*}}$	$0.005 \pm 0.003^{\text{b,*}}$	$833 \pm 494^{\text{b}}$	$2.0 \pm 1.1^{\text{ab}}$	$1.2 \pm 0.5^{\text{ab}}$
	TTA	n.d.	n.d.	n.d.	n.d.	n.d.
	TPAn-6	n.d.	n.d.	n.d.	n.d.	n.d.
	DPAn-6 ^{&}	$0.0004 \pm 0.0001^{\text{d,*}}$	$0.0001 \pm 0.00005^{\text{d,*}}$	$29 \pm 11^{\text{d,*}}$	$0.067 \pm 0.021^{\text{c}}$	$14.3 \pm 6.5^{\text{c}}$
	DPAn-6	ARA	n.d.	n.d.	n.d.	n.d.
DPAn-6		$0.013 \pm 0.007^{\text{f,*}}$	$1.6 \pm 0.6^{\text{f,*}}$	$1690 \pm 609^{\text{f,*}}$	$6.2 \pm 2.6^{\text{f}}$	$0.31 \pm 0.10^{\text{f}}$

Different superscript letters represent statistically different kinetic values between fatty acids and within a kinetic measure for each individual n-3 and n-6 PUFA biosynthetic pathway. Values are expressed as mean \pm SEM, $n = 8$. DGLA, dihomo- γ -linolenic acid.

[#]Represents significantly different kinetic values for an individual PUFA derived from DHA versus ALA, and DPAn-6 versus LNA precursors, $P < 0.05$.

*Represents significantly different kinetic values compared with n-3 PUFA biosynthetic pathway homologs for all n-6 PUFAs by t -test, $P < 0.05$.

[&] $n = 3$ for DPAn-6 kinetic parameters from LNA.

DISCUSSION

In the current study, we have demonstrated significant similarities in the kinetic parameters of synthesis-secretion for individual n-3 PUFAs produced from ALA, as well as n-6 PUFAs produced from LNA. For instance, the daily synthesis-secretion rate of DHA from plasma unesterified ALA was not different than SDA, 20:3n-3, 20:4n-3, EPA, DPAn-3, or THA, despite plasma DHA levels being 413-, 129-, 265-, 13-, 11-, and 126-fold higher, respectively. The significantly slower turnover and longer half-life of newly synthesized DHA from ALA compared with all other products of ALA likely explains the discrepancy between n-3 PUFA synthesis-secretion rates and plasma concentrations. This suggests varying levels of control, namely turnover, that maintains high plasma and tissue DHA levels while minimizing the levels of other n-3 PUFAs. However, because plasma turnover values may be determined by any or all tissue requirements (i.e., adipose, muscle, etc.) in the whole body, any conclusions on the turnover of specific PUFAs, such as DHA, must be made in reference to the whole body.

However, measures of downstream n-3 PUFA turnover from ALA can be difficult to interpret, as the tracer becomes diluted as it travels through the pathway and may not result in a true measure of DHA turnover. As a result, turnover and half-life of newly synthesized DHA from ALA by these calculations would be significantly underestimated and overestimated, respectively (14, 15). To address this,

we co-infused $^3\text{H}_5\text{-ALA}$ and $^{13}\text{C}_{22}\text{-DHA}$ to compare the turnover rate of DHA from plasma unesterified ALA compared with the turnover rate from plasma unesterified DHA. Kinetic parameters for DHA synthesis-secretion, turnover, and half-life represent the movement of plasma unesterified DHA into the total plasma DHA pool, including incorporation into phospholipid, triacylglycerol, cholesteryl ester, and free forms. As expected, turnover of DHA in the total plasma pool from the unesterified DHA pool was 130-fold faster and the half-life 200-fold shorter when compared with turnover and half-life determined from unesterified plasma ALA. These findings were supported by similar differences in the turnover (90-fold) and half-life (45-fold) of total newly synthesized DPAn-6 from unesterified plasma LNA compared to when determined directly from unesterified plasma DPAn-6. We expect this pattern of turnover rates to apply to other PUFAs, such as THA; however, this needs to be tested directly. Interestingly, turnover of total plasma ALA and DHA determined directly from the plasma unesterified pool were $12.8 \pm 2.1\%$ and $8.9 \pm 2.4\%$ per day, respectively, and were not statistically different. Similarly, we have previously determined the direct turnover of EPA to be $4.9 \pm 0.8\%$ per day by the same model (14).

Plasma total DHA was 128-fold higher than total THA and is comparable to previous plasma THA levels determined over a range of dietary ALA and DHA intakes (25). However, synthesis-secretion rates between DHA ($94 \pm$

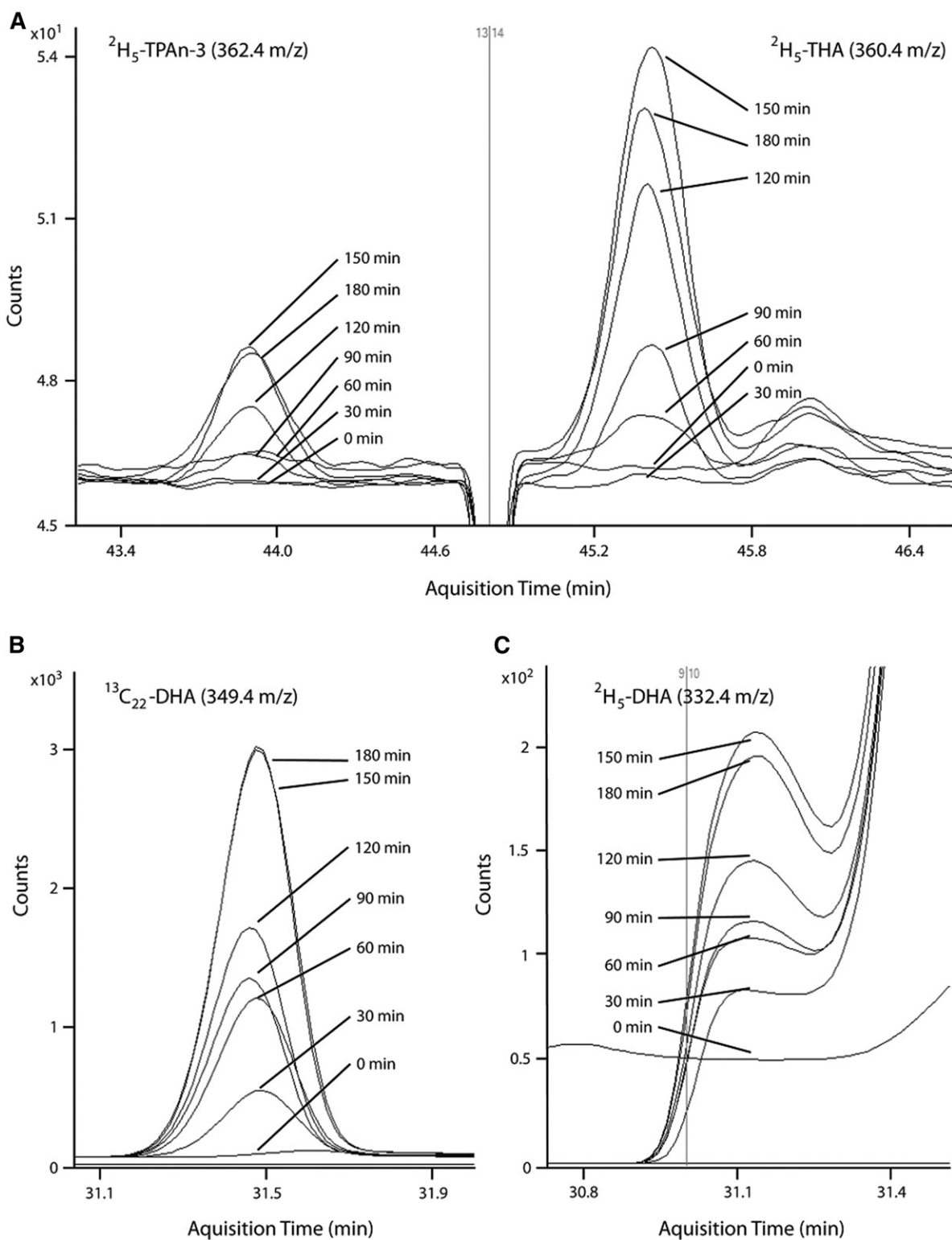


Fig. 3. Representative GC-MS chromatograms during 0–180 min infusion for total plasma $^2\text{H}_5$ -TPAn-3 and $^2\text{H}_5$ -THA (A), total plasma $^{13}\text{C}_{22}$ -DHA (B), and total plasma $^2\text{H}_5$ -DHA (C) ($n = 1$).

31 nmol/day) and THA (42 ± 13 nmol/day) were not different, suggesting that synthesis-secretion rates are unlikely to explain differences in plasma levels of these and other n-3 PUFAs. This identifies turnover of newly synthesized n-3 PUFAs, and not synthesis-secretion rates, as the likely mechanism responsible for determining blood and tissue

n-3 PUFA profiles. This is further supported by the synthesis rates of SDA, 20:3n-3, and 20:4n-3 that were similar to DHA, but with much faster turnovers (Table 2); they yield significantly lower total plasma levels (Fig. 1).

THA is believed to be the direct precursor to DHA (26) and any molecule of ALA converted to DHA must have

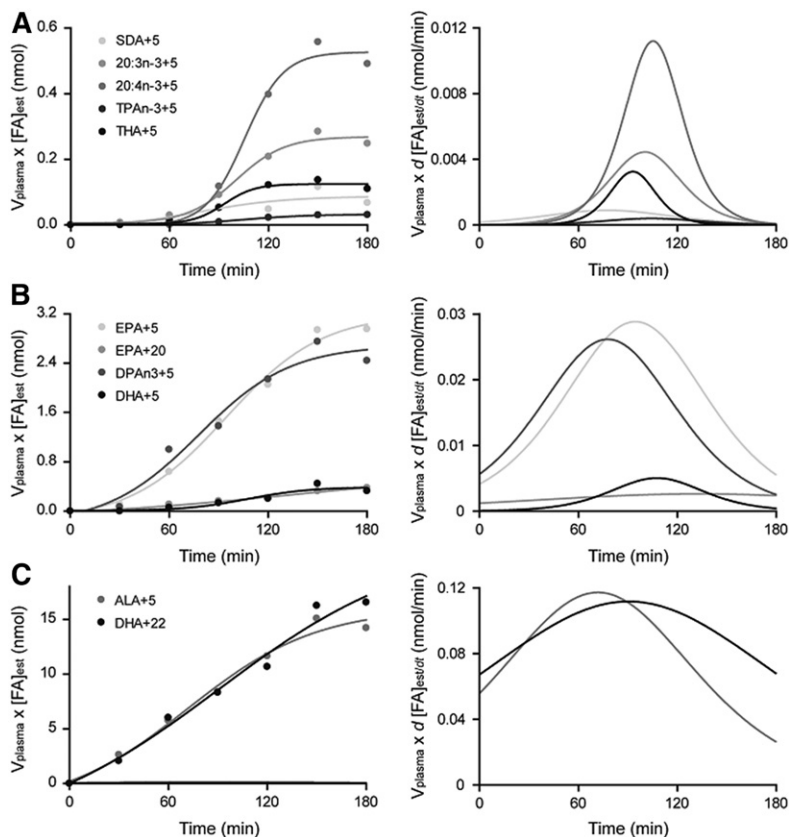


Fig. 4. Representative infusion curves and first derivatives for each labeled $^2\text{H}_5$ product of ALA and $^{13}\text{C}_{22}$ product of DHA, including: $^2\text{H}_5$ -SDA, $^2\text{H}_5$ -20:3n-3; $^2\text{H}_5$ -20:4n-3, $^2\text{H}_5$ -TPAn-3, and $^2\text{H}_5$ -THA (A); $^2\text{H}_5$ -EPA, $^{13}\text{C}_{22}$ -EPA, $^2\text{H}_5$ -DPAAn-3, and $^2\text{H}_5$ -DHA (B); and $^2\text{H}_5$ -ALA and $^{13}\text{C}_{22}$ -DHA (C) ($n = 1$).

been converted to THA first, thereby explaining the similar rates of synthesis-secretion. The same but reverse conclusion could be reached should THA actually be a product of DHA, as has been suggested in human MCF-7 cancer cell lines (27). In this well-designed study, cells were incubated in the presence of $^2\text{H}_5$ -ALA for between 24 and 72 h, and the appearance of downstream n-3 PUFA products was determined. The $^2\text{H}_5$ -DHA was detectable after 24 h and continued to increase until 72 h, and $^2\text{H}_5$ -THA was detectable beginning at 36 h and remained stable until 72 h. From this single dose of $^2\text{H}_5$ -ALA to the cells, the appearance of labeled DHA prior to the appearance of labeled THA indicates that THA may be a product of DHA. The 56-fold faster turnover of newly synthesized THA compared with DHA shown presently may help to partially explain the later appearance of THA in cell culture shown previously; however, it is unknown how rodent plasma THA turnover relates to human cell THA turnover and requires further testing. Future infusion studies including isotopically labeled THA would be vital in expanding our knowledge of how DHA and THA kinetics are comparable in vivo.

In humans, dietary washout of plasma EPA and DHA following 7 days of fish oil supplementation indicates half-lives from plasma triacylglycerols of 0.41 ± 0.19 days for EPA and 0.31 ± 0.04 days for DHA (28). Half-lives determined from this washout study very closely resemble the direct half-lives previously determined from our kinetic modeling for EPA (0.16 ± 0.03 days) (14) and in the current study for DHA (0.14 ± 0.04 days) in rodent models. Similarly, compartmental kinetic modeling has determined the half-life of

plasma DHA from orally dosed $^2\text{H}_5$ -ALA in humans consuming a beef-based diet to be 0.54 ± 0.17 days (8). Interestingly, turnover was higher when individuals consumed a fish-based diet (1.8 ± 0.5 days). Conversely, plasma half-lives determined from orally administered uniformly labeled ^{13}C -DHA in humans showed a decrease in plasma half-life following five months of fish oil supplementation (3.0 ± 0.2 days) compared with baseline (4.5 ± 0.4 days) (20). Relatively similar turnover rates when comparing rodents and humans are expected, as conversion of ALA to DHA in rodents by methodologies commonly employed in human populations has previously been shown to closely resemble that of humans (11). To date, human studies assessing DHA turnover and half-life must be assessed over many days following an oral dose and/or dietary manipulations that make it difficult to accurately account for contributions from oxidation and tissue storage. As such, future studies utilizing our infusion and kinetic modeling techniques could provide real-time measures of turnover and half-life in response to changes in dietary n-3 PUFA intakes. Furthermore, we recently showed that pregnant rats do not have higher daily synthesis-secretion rates compared with age-matched virgin controls (15). Combined with no change in whole-body DHA stores, this suggests a potential increase in the half-life of DHA during pregnancy as a means to increase DHA availability to the developing fetus, a question that could be answered with our current model.


The synthesis-secretion coefficients of all n-3 PUFAs from ALA were higher ($P < 0.05$) compared with each n-6 PUFA homolog from LNA. For example, the synthesis-secretion

coefficient for EPA of 0.068 ± 0.013 ml/min was more than 20-fold higher than the value for ARA of 0.003 ± 0.001 ml/min. Although a higher preference of desaturase and elongase enzymes for n-3 PUFAs over n-6 PUFAs has been demonstrated previously in vitro (29), to the best of our knowledge, this is the first in vivo study to demonstrate a similar preference of these enzymes for n-3 compared with n-6 PUFAs. However, after correcting for the much smaller plasma unesterified ALA versus LNA pool, the daily synthesis-secretion rates (nanomoles per day) of 20:3n-3, 20:4n-3, EPA, and DPAn-3 are not different than 20:2n-6, 20:3n-6, ARA, and 22:4n-6, respectively. Interestingly, the synthesis-secretion rate of DHA was 2-fold higher than DPAn-6, suggesting that a mechanism for downregulating the desaturation of 22:4n-6 to DPAn-6 exists independent of a similar downregulation in the n-3 PUFA homologs (DPAn-3 to DHA). This was supported by our inability to detect any $^{13}\text{C}_{18}$ labels in the 24-carbon n-6 PUFA intermediates, and the fact that DPAn-6 synthesis-secretion kinetic parameters were only measurable in three rodents, as $^{13}\text{C}_{18}$ -DPAn-6 was not detectable in the other five animals. Similarly, the amount of plasma DHA being formed directly from plasma unesterified DHA ($11,780 \pm 3,147$ nmol/day) was 5-fold higher than plasma DPAn-6 being formed from plasma unesterified DPAn-6 ($1,690 \pm 609$ nmol/day). As turnover of DPAn-6 and DHA from plasma unesterified DPAn-6 and DHA, respectively, were not different, a lower rate of synthesis-secretion of DPAn-6 compared with DHA is the likely mechanism, and we have demonstrated this previously (13).

Elongation of very long-chain 2 (Elovl2) has a higher affinity for substrates of the n-3 PUFA pathway over the n-6 PUFA pathway, specifically a 2.5-fold higher affinity for DPAn-3 over 22:4n-6 for elongation to TPAn-3 and TTA, respectively (29). The higher synthesis-secretion coefficients for the n-3 PUFAs in our study support these findings, as does the inability to detect any synthesis-secretion of TTA or TPAn-6, and the significantly lower DPAn-6 synthesis-secretion compared with DHA. Furthermore, Elovl2 has a 4.5-fold higher affinity for EPA compared with ARA (29), suggesting that, beginning at EPA and continuing with DPAn-3, the PUFA biosynthesis pathways are much more capable of synthesizing DHA over DPAn-6 despite similar synthesis-secretion rates of metabolic precursors. Interestingly, although turnover of 22:4n-6 was similar to DPAn-3, the lack of significant conversion to downstream n-6 PUFAs indicates that 22:4n-6 may be a source for β -oxidation or 22:4n-6-derived docosanoids (30, 31). Co-infusion of labeled n-3 and n-6 PUFA homologs in this section of the pathway, such as EPA versus ARA or DPAn-3 versus 22:4n-6, could clearly identify the presence of a faster turnover to DHA versus DPAn-6, respectively.

Presently, we also demonstrate 373 ± 121 nmol/day retroconversion of DHA to EPA that was equal to the determined 369 ± 86 nmol/day synthesis-secretion of EPA from ALA. Surprisingly, these nearly identical synthesis-secretion rates are reached despite the approximately two times higher synthesis-secretion coefficient of EPA from DHA (0.13 ± 0.03 ml/min) compared with EPA from ALA ($0.068 \pm$

0.013 ml/min). However, it must be noted that we detected some $^{13}\text{C}_{20}$ -EPA contamination in the infusate equal to each rat receiving approximately 8 nmol of the $^{13}\text{C}_{20}$ -EPA contaminant (data not shown). Therefore, although the relative contribution of EPA from DHA of 50% is very close to the 39% contribution previously determined by isotope ratio MS (22), the 1.3 times higher EPA synthesis-secretion rates determined from DHA presently may be explained by the $^{13}\text{C}_{20}$ contaminant. Therefore, due to this impurity, we are unable to establish direct evidence of retroconversion in this model, as it is possible that all that was measured is an artifact. Conversely, retroconversion of DPAn-6 to ARA was not detectable under the current study parameters and is supportive of our previous findings (22). Future studies assessing the contribution of DHA compared with ALA to increases in plasma EPA following dietary DHA in a co-infusion model could quantify the rates of EPA synthesis-secretion from the two plasma unesterified sources.

In conclusion, despite similar rates of synthesis-secretion from ALA, we demonstrate large differences in turnover of DHA compared with other low plasma level n-3 PUFAs, such as THA, SDA, and others. These differences suggest that turnover and not synthesis may be a primary determinant for tissue and blood n-3 PUFA levels. In addition, comparing the kinetic parameters between n-3 and n-6 PUFA homologs supports the relatively higher affinity of elongase enzymes for 22-carbon n-3 PUFAs, and may explain the higher synthesis-secretion rates of DHA versus DPAn-6. Finally, by including both $^{13}\text{C}_{22}$ -DHA and $^2\text{H}_5$ -ALA in a co-infusion model, we were able to show that previous estimates of DHA turnover from ALA were significant underestimates of true DHA turnover, and this co-infusion model will allow for real-time direct determinations of DHA turnover and half-life values under numerous experimental conditions. 

REFERENCES

- Burdge, G. C., Y. E. Finnegan, A. M. Minihane, C. M. Williams, and S. A. Wootton. 2003. Effect of altered dietary n-3 fatty acid intake upon plasma lipid fatty acid composition, conversion of [^{13}C] alpha-linolenic acid to longer-chain fatty acids and partitioning towards beta-oxidation in older men. *Br. J. Nutr.* **90**: 311–321.
- Burdge, G. C., A. E. Jones, and S. A. Wootton. 2002. Eicosapentaenoic and docosapentaenoic acids are the principal products of alpha-linolenic acid metabolism in young men. *Br. J. Nutr.* **88**: 355–363.
- Burdge, G. C., and S. A. Wootton. 2002. Conversion of alpha-linolenic acid to eicosapentaenoic, docosapentaenoic and docosahexaenoic acids in young women. *Br. J. Nutr.* **88**: 411–420.
- Emken, E. A., R. O. Adlof, S. M. Duval, and G. J. Nelson. 1999. Effect of dietary docosahexaenoic acid on desaturation and uptake in vivo of isotope-labeled oleic, linoleic, and linolenic acids by male subjects. *Lipids*. **34**: 785–791.
- Emken, E. A., R. O. Adlof, and R. M. Gulley. 1994. Dietary linoleic acid influences desaturation and acylation of deuterium-labeled linoleic and linolenic acids in young adult males. *Biochim. Biophys. Acta*. **1213**: 277–288.
- Mayes, C., G. C. Burdge, A. Bingham, J. L. Murphy, R. Tubman, and S. A. Wootton. 2006. Variation in [^{13}C] alpha linolenic acid absorption, beta-oxidation and conversion to docosahexaenoic acid in the pre-term infant fed a DHA-enriched formula. *Pediatr. Res.* **59**: 271–275.

7. McCloy, U., M. A. Ryan, P. B. Pencharz, R. J. Ross, and S. C. Cunnane. 2004. A comparison of the metabolism of eighteen-carbon ¹³C-unsaturated fatty acids in healthy women. *J. Lipid Res.* **45**: 474–485.
8. Pawlosky, R. J., J. R. Hibbeln, Y. Lin, S. Goodson, P. Riggs, N. Sebring, G. L. Brown, and N. Salem, Jr. 2003. Effects of beef- and fish-based diets on the kinetics of n-3 fatty acid metabolism in human subjects. *Am. J. Clin. Nutr.* **77**: 565–572.
9. Pawlosky, R. J., J. R. Hibbeln, J. A. Novotny, and N. Salem, Jr. 2001. Physiological compartmental analysis of alpha-linolenic acid metabolism in adult humans. *J. Lipid Res.* **42**: 1257–1265.
10. Pawlosky, R. J., H. W. Sprecher, and N. Salem, Jr. 1992. High sensitivity negative ion GC-MS method for detection of desaturated and chain-elongated products of deuterated linoleic and linolenic acids. *J. Lipid Res.* **33**: 1711–1717.
11. Domenichiello, A. F., C. T. Chen, M. O. Trepanier, P. M. Stavro, and R. P. Bazinet. 2014. Whole body synthesis rates of DHA from alpha-linolenic acid are greater than brain DHA accretion and uptake rates in adult rats. *J. Lipid Res.* **55**: 62–74.
12. Domenichiello, A. F., A. P. Kitson, C. T. Chen, M. O. Trepanier, P. M. Stavro, and R. P. Bazinet. 2016. The effect of linoleic acid on the whole body synthesis rates of polyunsaturated fatty acids from alpha-linolenic acid and linoleic acid in free-living rats. *J. Nutr. Biochem.* **30**: 167–176.
13. Domenichiello, A. F., A. P. Kitson, A. H. Metherel, C. T. Chen, K. E. Hopperton, P. M. Stavro, and R. P. Bazinet. 2017. Whole-body docosahexaenoic acid synthesis-secretion rates in rats are constant across a large range of dietary alpha-linolenic acid intakes. *J. Nutr.* **147**: 37–44.
14. Metherel, A. H., A. F. Domenichiello, A. P. Kitson, K. E. Hopperton, and R. P. Bazinet. 2016. Whole-body DHA synthesis-secretion kinetics from plasma eicosapentaenoic acid and alpha-linolenic acid in the free-living rat. *Biochim. Biophys. Acta.* **1861**: 997–1004.
15. Metherel, A. H., A. P. Kitson, A. F. Domenichiello, R. J. S. Lacombe, K. E. Hopperton, M. O. Trepanier, S. M. Alashmali, L. Lin, and R. P. Bazinet. 2017. Maternal liver docosahexaenoic acid (DHA) stores are increased via higher serum unesterified DHA uptake in pregnant long Evans rats. *J. Nutr. Biochem.* **46**: 143–150.
16. Rapoport, S. I., M. Igarashi, and F. Gao. 2010. Quantitative contributions of diet and liver synthesis to docosahexaenoic acid homeostasis. *Prostaglandins Leukot. Essent. Fatty Acids.* **82**: 273–276.
17. Blasbalg, T. L., J. R. Hibbeln, C. E. Ramsden, S. F. Majchrzak, and R. R. Rawlings. 2011. Changes in consumption of omega-3 and omega-6 fatty acids in the United States during the 20th century. *Am. J. Clin. Nutr.* **93**: 950–962.
18. Hussein, N., E. Ah-Sing, P. Wilkinson, C. Leach, B. A. Griffin, and D. J. Millward. 2005. Long-chain conversion of [¹³C]linoleic acid and alpha-linolenic acid in response to marked changes in their dietary intake in men. *J. Lipid Res.* **46**: 269–280.
19. Salem, N., Jr., R. Pawlosky, B. Wegher, and J. Hibbeln. 1999. In vivo conversion of linoleic acid to arachidonic acid in human adults. *Prostaglandins Leukot. Essent. Fatty Acids.* **60**: 407–410.
20. Plourde, M., R. Chouinard-Watkins, C. Rioux-Perreault, M. Fortier, M. T. Dang, M. J. Allard, J. Tremblay-Mercier, Y. Zhang, P. Lawrence, M. C. Vohl, et al. 2014. Kinetics of ¹³C-DHA before and during fish-oil supplementation in healthy older individuals. *Am. J. Clin. Nutr.* **100**: 105–112.
21. DeMar, J. C., Jr., K. Ma, J. M. Bell, and S. I. Rapoport. 2004. Half-lives of docosahexaenoic acid in rat brain phospholipids are prolonged by 15 weeks of nutritional deprivation of n-3 polyunsaturated fatty acids. *J. Neurochem.* **91**: 1125–1137.
22. Metherel, A. H., R. Chouinard-Watkins, M. Trepanier, R. J. S. Lacombe, and R. P. Bazinet. 2017. Retroconversion is a minor contributor to increases in eicosapentaenoic acid following docosahexaenoic acid feeding as determined by compound specific isotope analysis in rat liver. *Nutr. Metab. (Lond.)* **14**: 75.
23. Schreihöfer, A. M., C. D. Hair, and D. W. Stepp. 2005. Reduced plasma volume and mesenteric vascular reactivity in obese Zucker rats. *Am. J. Physiol. Regul. Integr. Comp. Physiol.* **288**: R253–R261.
24. Folch, J., M. Lees, and G. H. Sloane Stanley. 1957. A simple method for the isolation and purification of total lipides from animal tissues. *J. Biol. Chem.* **226**: 497–509.
25. Metherel, A. H., A. F. Domenichiello, A. P. Kitson, Y. H. Lin, and R. P. Bazinet. 2017. Serum n-3 tetracosapentaenoic acid and tetracosahexaenoic acid increase following higher dietary alpha-linolenic acid but not docosahexaenoic acid. *Lipids.* **52**: 167–172.
26. Voss, A., M. Reinhart, S. Sankarappa, and H. Sprecher. 1991. The metabolism of 7,10,13,16,19-docosapentaenoic acid to 4,7,10,13,16,19-docosahexaenoic acid in rat liver is independent of a 4-desaturase. *J. Biol. Chem.* **266**: 19995–20000.
27. Park, H. G., W. J. Park, K. S. Kothapalli, and J. T. Brenna. 2015. The fatty acid desaturase 2 (FADS2) gene product catalyzes Delta4 desaturation to yield n-3 docosahexaenoic acid and n-6 docosapentaenoic acid in human cells. *FASEB J.* **29**: 3911–3919.
28. Zuijdgeest-van Leeuwen, S. D., P. C. Dagnelie, T. Rietveld, J. W. van den Berg, and J. H. Wilson. 1999. Incorporation and washout of orally administered n-3 fatty acid ethyl esters in different plasma lipid fractions. *Br. J. Nutr.* **82**: 481–488.
29. Gregory, M. K., R. A. Gibson, R. J. Cook-Johnson, L. G. Cleland, and M. J. James. 2011. Elongase reactions as control points in long-chain polyunsaturated fatty acid synthesis. *PLoS One.* **6**: e29662.
30. Kopf, P. G., D. X. Zhang, K. M. Gauthier, K. Nithipatikom, X. Y. Yi, J. R. Falck, and W. B. Campbell. 2010. Adrenic acid metabolites as endogenous endothelium-derived and zona glomerulosa-derived hyperpolarizing factors. *Hypertension.* **55**: 547–554.
31. Yi, X. Y., K. M. Gauthier, L. Cui, K. Nithipatikom, J. R. Falck, and W. B. Campbell. 2007. Metabolism of adrenic acid to vasodilatory 1alpha,1beta-dihomo-epoxyeicosatrienoic acids by bovine coronary arteries. *Am. J. Physiol. Heart Circ. Physiol.* **292**: H2265–H2274.